Study of ultrasonic thermometry based on ultrasonic time-of-flight measurement

Cite as: AIP Advances **6**, 035006 (2016); https://doi.org/10.1063/1.4943676
Submitted: 07 January 2016 • Accepted: 29 February 2016 • Published Online: 07 March 2016

Ruixi Jia, Qingyu Xiong, Lijie Wang, et al.

AIP ADVANCES **6**, 035006 (2016)

Study of ultrasonic thermometry based on ultrasonic time-of-flight measurement

Ruixi Jia,[1,2] Qingyu Xiong,[1,3,a] Lijie Wang,[1,2] Kai Wang,[1] Xuehua Shen,[1] Shan Liang,[1] and Xin Shi[1]
[1]*Key Laboratory of Dependable Service Computing in Cyber Physical Society, MOE, Chongqing 400044, China*
[2]*School of Automation, Chongqing University, Chongqing 400044, China*
[3]*School of Software Engineering, Chongqing University, Chongqing 400044, China*

(Received 7 January 2016; accepted 29 February 2016; published online 7 March 2016)

Ultrasonic thermometry is a kind of acoustic pyrometry and it has been evolving as a new temperature measurement technology for various environment. However, the accurate measurement of the ultrasonic time-of-flight is the key for ultrasonic thermometry. In this paper, we study the ultrasonic thermometry technique based on ultrasonic time-of-flight measurement with a pair of ultrasonic transducers for transmitting and receiving signal. The ultrasonic transducers are installed in a single path which ultrasonic travels. In order to validate the performance of ultrasonic thermometry, we make a contrast about the absolute error between the measured temperature value and the practical one. With and without heater source, the experimental results indicate ultrasonic thermometry has high precision of temperature measurement. [http://dx.doi.org/10.1063/1.4943676]

I. INTRODUCTION

Ultrasonic thermometry is a kind of acoustic pyrometry and it has been evolving as a new temperature measurement technology for various environment, in which the traditional temperature measurement methods have failed to operate satisfactorily, such as mercury thermometer, thermocouple, thermal resistance, infrared thermometry and optical fiber pyrometer. The basic principle of ultrasonic thermometry is that, based on the relationship between the velocity of ultrasound and the properties of the medium, which the ultrasound travels through, the average temperature along its travel path can easily be calculated after measuring the ultrasound velocity between the ultrasonic transmitter and receiver.[1–4] In the meanwhile, the ultrasonic speed is determined by distance ultrasonic travels and the ultrasonic time-of-flight(UTOF). For specific circumstance, the medium composition and the distance are easily obtained. Then, the ultrasonic speed is gained. Thus, the temperature can be inferred from the UTOF. So, the accurate measurement of the UTOF is the key for ultrasonic thermometry.

In this paper, we study the ultrasonic thermometry technique based on UTOF measurement by fitting the rising phases of double echo envelopes using double excitations. A pair of ultrasonic transducers for transmitting and receiving are placed in a single path. Under the condition of medium of air, with and without heater source, we make a contrast about the absolute error between the measured temperature value and the practical one. With and without heater source, the experimental results indicate ultrasonic thermometry has high precision of temperature measurement.

This paper is organized as follows. Section II describes the basic principle of ultrasonic thermometry. Section III focuses on the algorithm of UTOF measurement by fitting the rising phases of

[a]Corresponding author E-mail address: cquxqy@163.com

double echo envelopes using double excitations. Section IV shows the experiment results. Conclusion and future work are drawn in Section V.

II. THE BASIC PRINCIPLE OF ULTRASONIC THERMOMETRY

Under the condition of ideal gas at a constant pressure, according to Boyle's law, the relationship of ultrasonic speed and temperature is regarded as[5,6]

$$c = \sqrt{\frac{\gamma RT}{M}} = Z\sqrt{T} \tag{1}$$

where c is the speed of ultrasonic, R is the specific gas constant of the intervening air medium, T is the absolute temperature (K), M is the average molecular weight of the gas molecules and $\gamma = C_p/C_v$, where C_p is the heat capacity of the gas at constant pressure and C_v is the heat capacity of gas at constant volume. For different gas, R, M and γ are fixed constants. So, Z is 20.05 when intervening medium is air and can be described as

$$Z = \sqrt{\frac{\gamma R}{M}} \tag{2}$$

If ultrasonic speed c and the type of gas are known, then the temperature T is expressed as

$$T = (\frac{c}{Z})^2 \tag{3}$$

Before experiment, the location of ultrasonic transducers is known. So, the distance L between two ultrasonic transducers is acquired. According to the correlativity of ultrasonic speed c, UTOF and distance L, we can get

$$c = \frac{L}{\mathrm{UTOF}} \tag{4}$$

combine Eq.(3) and Eq.(4), the average temperature T (°C) of the path ultrasonic travels is acquired from Eq.(5).

$$T = \frac{1}{Z^2}(\frac{L}{\mathrm{UTOF}})^2 - 273.15 \tag{5}$$

III. THE ALGORITHM OF ULTRASONIC THERMOMETRY

A. The ultrasonic thermometry system

The composition structure diagram of entire the ultrasonic thermometry system is shown in Fig. 1. It consists of Tektronix signal generator, ultrasonic transmitting transducer, thermocouple 1, thermocouple 2, digital temperature indicator MIK100, digital temperature indicator XMT618, ultrasonic receiving transducer, signal conditioning, Tektronix oscilloscope, ultrasonic signal processing with PC, optical bench and other parts. Experimental setup of the ultrasonic thermometry is displayed in Fig. 2 and Fig. 3.

In order to get a uniform temperature, we use an environmental chamber to have the absolute control of temperature and other environmental variables. The thermocouple 1 and thermocouple 2 are connected to digital temperature indicator MIK100 and digital temperature indicator XMT618. Both temperature indicators have high measurement precision. Before measurement, thermocouples are calibrated so as to obtain accurate practical temperature. The working principle of the ultrasonic thermometry measurement system is as follows: firstly, a pair of ultrasonic transducer for transmitting and receiving signal are placed in optical bench. Secondly, 8 and 12 sine pulses emitted respectively from Tektronix signal generator, pass through ultrasonic drive circuit, to motivate the ultrasonic transmitting transducer which converts electrical energy into sound energy and transmits it. When the sound encounters ultrasonic receiving transducer, ultrasonic receiving transducer receives the ultrasonic sound and converts sound energy into electrical energy (echo signal). Thirdly,

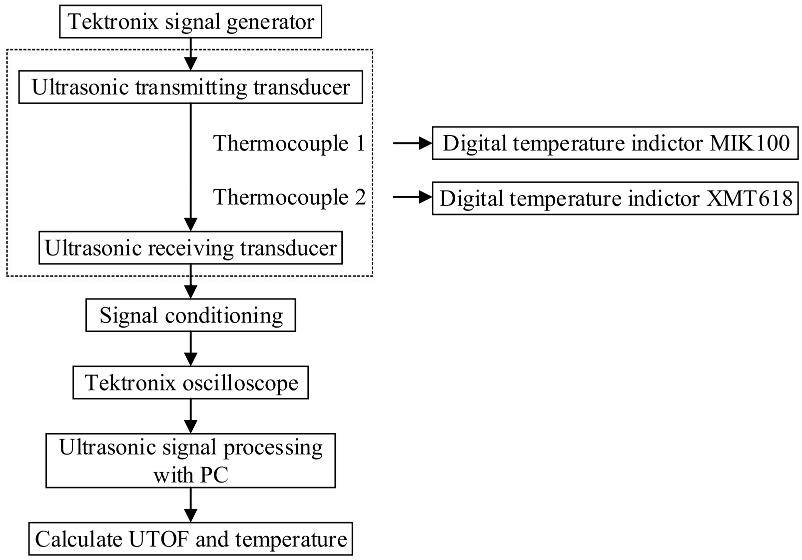

FIG. 1. Composition structure diagram of ultrasonic thermometry system.

the echo signal processed by signal conditioning circuit will be collected to PC through the Tektronix oscilloscope. The logical connection of Tektronix signal generator, Tektronix oscilloscope and PC is described in LabVIEW software platform. Finally, using MATLAB software platform, PC with LabVIEW software, will capture, store, display, analyze and calculate the UTOF and the average temperature.

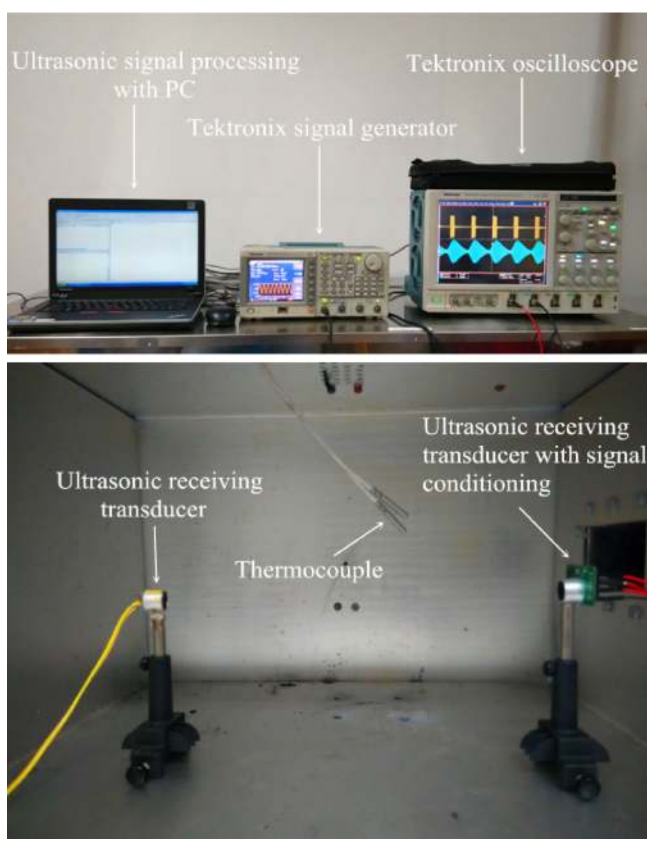

FIG. 2. Experimental setup of the ultrasonic thermometry without heater source.

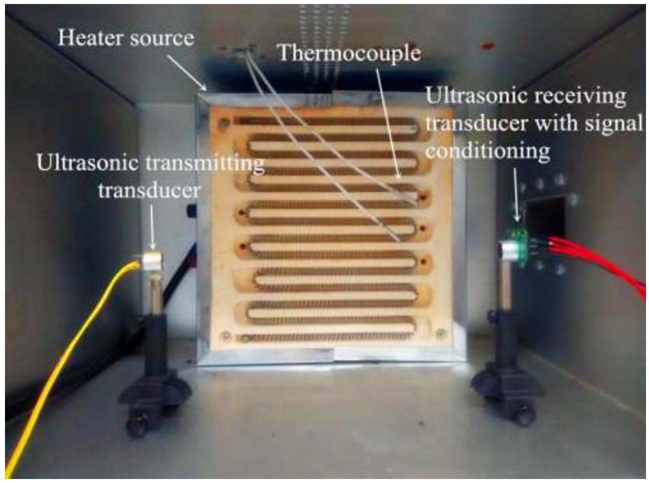

FIG. 3. Experimental setup of the ultrasonic thermometry with heater source.

B. Extracting echo signal envelope

Echo signal envelope describes the whole trend of echo waveform which is helpful to obtain the UTOF. Hilbert transform is an efficient method to extract the echo signal envelope.[7] The detail method is:

For a continuous time signal $x(t)$, its Hilbert transform $h(t)$ is defined as

$$h(t) = H\{x(t)\} = \frac{1}{\pi}\int_{-\infty}^{+\infty}\frac{x(\tau)}{t-\tau}d\tau \tag{6}$$

The analytical $z(t)$ is given as

$$z(t) = x(t) + jh(t) \tag{7}$$

$z(t)$ is a plural signal and its amplitude $A(t)$ and phase $\varphi(t)$ are expressed as

$$z(t) = A(t)e^{j\varphi(t)} \tag{8}$$

where

$$A(t) = \sqrt{[x(t)]^2 + [h(t)]^2} \tag{9}$$

$$\varphi(t) = arctg[\frac{h(t)}{x(t)}] \tag{10}$$

where $A(t)$ is the envelope of given signal $x(t)$.

C. The mathematical model of ultrasonic echo envelope

For air piezoelectric 40LT-16 and 40LR-16, the echo wave distortion will occur when excitation pulse number is over 50.[8] Here, we use double sine waves as excitation pulses, one's number is 8, another is 12, because echo wave distortion will not occur and echo response will be rapid relatively.

Based on the UTOF measurement system, air piezoelectric 40LT-16 as ultrasonic transmitting transducer, air piezoelectric 40LR-16 as ultrasonic receiving transducer, air as the transmitting medium, data sampling frequency is 1 MHz. Using the Hilbert transform method, according to the practical ultrasonic echo signals, their corresponding envelopes are shown in Fig. 4 and Fig. 5.

Fig. 6 expresses the practical echo envelopes with 8 and 12 sine pulses.

L. Angrisani et al.[9] used an echo envelope mathematical model, it is expressed as

$$V(t) = A_0(\frac{t-\lambda}{\delta})^{\alpha}\exp(\frac{t-\lambda}{\delta}) \tag{11}$$

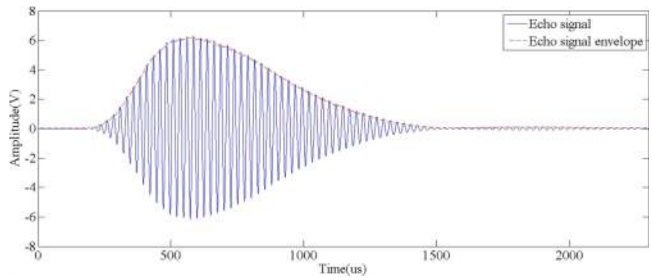

FIG. 4. The practical ultrasonic echo and its envelope when the excitation sine pulse number is 8.

where A_0,λ,δ, and α are model parameters. A_0 is the echo amplitude, α and δ are distinct to the specific ultrasonic transducer, and λ is the desired UTOF.

According to Fig. 4 and Fig. 5, there are two main phases in the ultrasonic echo signal, rising phase and falling phase. Rising phase is that ultrasonic transmitting transducer chip is forced to vibrate by the excitation signal and the signal amplitude V is rising. After the ultrasonic echo amplitude reaches the maximum value V_m (peak value), it is decreasing gradually and the falling phase begins until the echo amplitude is close to 0 V.

D. Determining UTOF by fitting the rising phases of double echo envelopes using double excitations

Fig. 7 shows the practical ultrasonic echo waves with 8 and 12 sine pulses.

UTOF is the time when ultrasonic travels through a path between ultrasonic transmitting transducer and ultrasonic receiving transducer. So, any time interval when ultrasonic transmitting transducer emits each sine pulse and ultrasonic receiving transducer detects the corresponding echo response can be used to estimate UTOF. For the same system, judging from Fig. 7, the two echo waves are basically the same in the first 8 echo responses and they become different and separated after the echo response of the eighth sine pulse. Therefore, in echo waves, there exists a separated point which is corresponding to the echo response of the eighth sine pulse. Here, we use the time interval of eighth sine pulse and its echo response to estimate UTOF. The start time is assumed the moment when ultrasonic transmitting transducer emits the eighth sine pulse, the end time is the moment when ultrasonic receiving transducer detects the corresponding echo response. This time interval or UTOF are relative values and should be changed into absolute values when they are calculated.

If the separated point in echo waves can be confirmed, then it will be easy to determine UTOF. But, from Fig. 7, the separated point is difficult to be found in echo waves due to echo waves' complexity.

Similarly, the echo envelopes have the same tendency with echo waves. Moreover, echo envelopes are basically monotonous curves and only have rising phase and falling phase. It is easy to find the separated point in echo envelopes.

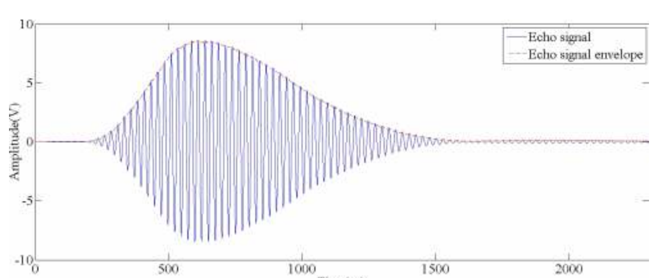

FIG. 5. The practical ultrasonic echo and its envelope when the excitation sine pulse number is 12.

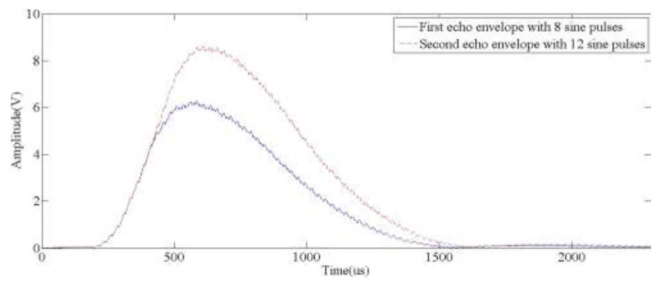

FIG. 6. The practical ultrasonic echo envelopes with 8 and 12 sine pulses.

However, from Fig. 6, it is hard to confirm the separated point directly because of the practical ultrasonic echo envelopes' non-smooth.

Assuming that the start time when ultrasonic transmitting transducer emits the eighth sine pulse is origin coordinate, the separated point is corresponding UTOF. Fig. 8 describes the actual location of separated point in practical echo envelopes. From Fig. 8, the separated point only exists in the rising phase of echo envelope and it is located between 50% of V_m (peak value) of the practical echo with 8 sine pulses to 75%. T_a and T_b are the horizontal ordinates of 50% of V_m and 75% of V_m. So, the UTOF is located between T_a and T_b.

Eq.(11) is an echo envelope mathematical model. For a practical echo envelope, the parameters of A_0,λ,δ and α are fixed. Therefore, if the two practical echo envelopes' parameters can be obtained, then, using the mathematical model in Eq.(11), we can acquire two corresponding curves. Thus, the separated point and the UTOF are easy to determine.

In order to gain the practical echo envelopes' parameters, it is feasible to use the mathematical model to fit the rising phases of the practical double echo envelopes in Fig. 6. Then, with the parameters estimated and the mathematical model, we can get two fitted envelopes and confirm the separated point and UTOF.

Particle Swarm Optimization (PSO),[10] is a valid algorithm to estimate parameters in mathematical model and acquire optimal echo envelopes' parameters because of its simple structure, ease of realization and ability to quickly reach the global optimal solution. It looks for the best solution using particles that consists of a swarm moving around in the search space. In PSO, there are two important parameters named position and velocity. The i^{th} particle's position X_i and velocity V_i in d-dimensional search space can be represented as $X_i = (x_{i1}, \ \ldots, \ x_{id})$ and $V_i = (v_{i1}, \ \ldots, \ v_{id})$, respectively. The other two important parameters are P_{best} and G_{best}. P_{best} and G_{best} mean the each particle's best solution and the swarm's fittest particle. Judging from own flying experience and information provided by other particles, each individual particle in the search space is adjusted dynamically. The swarm's global best solution is achieved simply by adjusting the trajectory of each individual toward its own best location and the best particle of the entire swarm at each iteration. For a given fitness function, P_{best} at time t is given as $P_{bi} = (p_{bi1}, \ \ldots, \ p_{bid})$ and G_{best} at the same time t is defined as $P_g = (p_{g1}, \ \ldots, \ p_{gd})$. Moreover, the particle's position and velocity are initialized randomly in PSO algorithm. Each particle's fitness value can be calculated. If the current

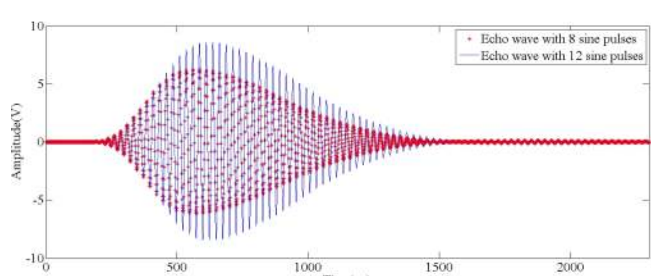

FIG. 7. The practical ultrasonic echo waves with 8 and 12 sine wave pulses.

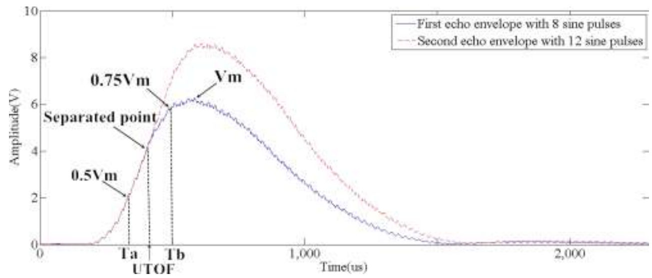

FIG. 8. The location of separated point in practical echo envelopes.

fitness value is better than P_{best}, this value will be set as the new P_{best}. G_{best} is the best fitness value of all the particles. The new velocities and positions of the particles for the next fitness evaluation can be updated according to Eq.(12) and (13). This process is still repeated until reaching the maximum iteration.

$$v_{id}(t+1) = \omega v_{id}(t) + r_1 c_1(p_{id} - x_{id}(t)) + r_2 c_2(p_{gd} - x_{id}(t)) \tag{12}$$

$$x(t+1) = x_{id}(t) + v_{id}(t+1) \tag{13}$$

where v_{id} is the velocity of d^{th} dimension of i^{th} particle, ω, r_1 and r_2 are constants. c_1 and c_2 are uniformly distributed random numbers with values between 0 and 1.

PSO algorithm parameters are defined as follows: the particle's number is 50, the dimension of the problem is 4, the number of iteration is 120 and ω, r_1 and r_2 are set to 1, 2 and 2.

The important performance metric of fitting the practical ultrasonic echo envelopes is the minimum error, which means the fitted one is almost the same with the practical one. So, here, we use the least-square criterion to build the fitness function (subjective function). It is defined as

$$f(\theta^{(j)}) = \sum_{i=a}^{i=b} [V(\theta^{(j)}) - V'(i)]^2 \tag{14}$$

where θ is the feature vector of ultrasonic echo envelope mathematical model, $\theta = (A_0, \lambda, \delta, \alpha)$, $V(\theta^{(j)})$ is the j^{th} iteration's ultrasonic echo envelope mathematical model, $V'(i)$ is the practical ultrasonic echo envelope data and the fitting interval, $[a, b]$, is from the origin of coordinates to the peak value of the practical ultrasonic echo envelope with 8 sine pulse.

Based on the fitness function, during the process of iteration, the feature vector θ is estimated when $f(\theta^{(j)})$ reaches the minimum value. Then, with the mathematical model of echo envelope, we can get two fitted envelopes. Hence, the separated point, the UTOF and the average temperature in the single path are worked out. The flowchart of PSO algorithm is shown in Fig. 9.

In PSO algorithm, the fitness function's parameters are the constraints of the problem and they are expressed as

$$A_{\min} \leq A_0 \leq A_{\max} \tag{15}$$

$$\lambda_{\min} \leq \lambda \leq \lambda_{\max} \tag{16}$$

$$\delta_{\min} \leq \delta \leq \delta_{\max} \tag{17}$$

$$\alpha_{\min} \leq \alpha \leq \alpha_{\max} \tag{18}$$

IV. EXPERIMENT RESULTS

The interval of the fitness function's parameters are set to [0 V, 10 V] for A_0, [10 us, 1000 us] for λ, [70, 160] for δ and [1, 6] for α.

Base on the UTOF measurement system and the PSO algorithm proposed, the practical echo envelopes and the fitted ones with 8 and 12 sine pulses are shown in Fig. 10 and Fig. 11.

Judging from Fig. 10 and Fig. 11, ignoring the falling phases, the algorithm presented precisely fits the rising phases of double echo envelopes with 8 and 12 sine pulses. Fig. 12 expresses the fitted

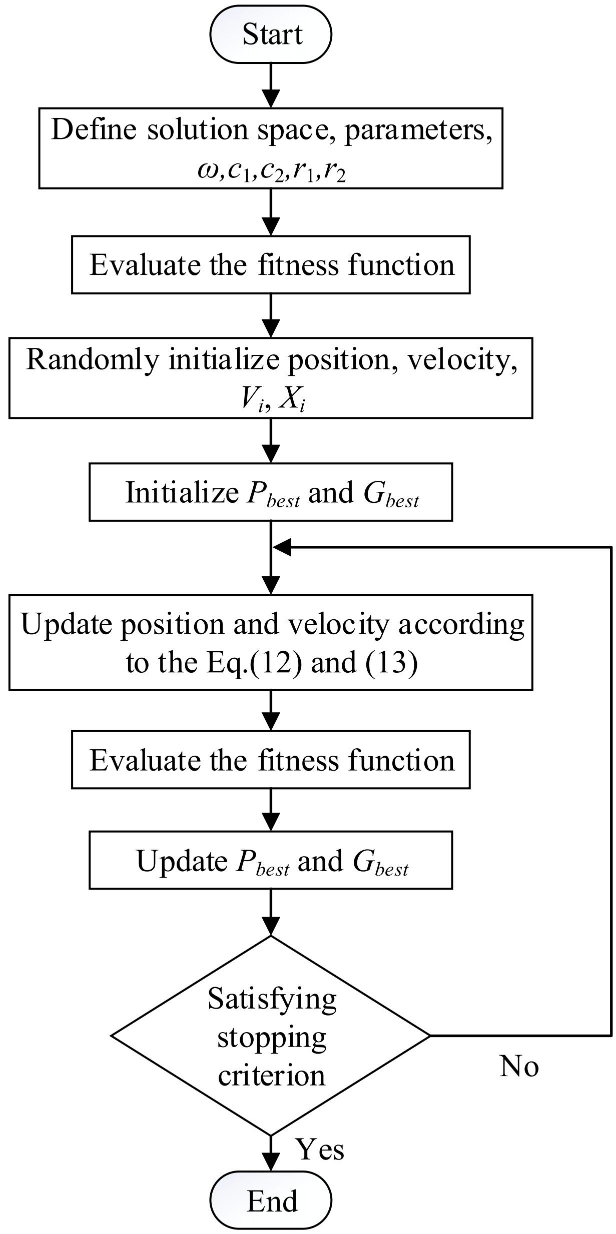

FIG. 9. The flowchart of PSO algorithm.

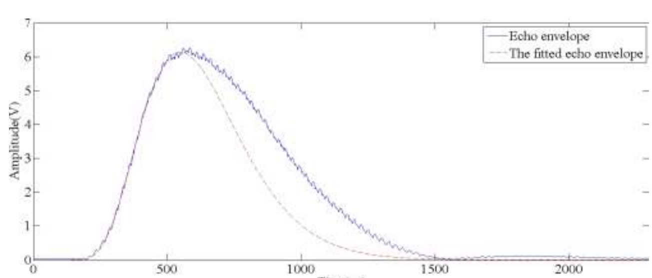

FIG. 10. The practical echo envelope and the fitted one with 8 sine pulses.

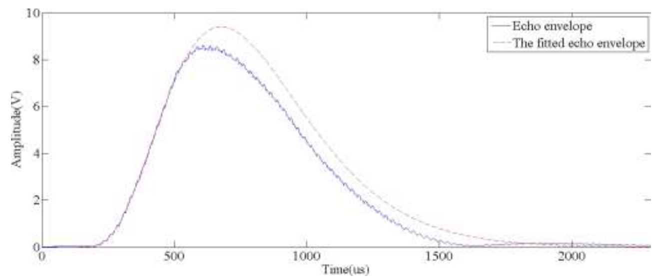

FIG. 11. The practical echo envelope and the fitted one with 12 sine pulses.

echo envelopes with 8 and 12 sine pulses. Compared with Fig. 6, the echo envelopes are smooth and the separated point is easy to find out.

θ' and θ'' are the estimated envelope feature vectors with 8 and 12 sine pulses and they are shown as

$$\theta' = (A_0', \alpha', \delta', \lambda') \tag{19}$$

$$\theta'' = (A_0'', \alpha'', \delta'', \lambda'') \tag{20}$$

The two fitted echo envelopes are described as

$$V'(t) = A_0'(\frac{t-\lambda'}{\delta'})^{\alpha'} \exp(\frac{t-\lambda'}{\delta'}) \tag{21}$$

$$V''(t) = A_0''(\frac{t-\lambda''}{\delta''})^{\alpha''} \exp(\frac{t-\lambda''}{\delta''}) \tag{22}$$

The difference ΔV is defined as

$$\Delta V = V'(t) - V''(t) \tag{23}$$

As previously mentioned, the separated point is located in the range of 50% of V_m (peak value) of the practical echo with 8 sine pulses to 75%. Therefore, in this range, when ΔV equals to 0, the corresponding horizontal ordinate is the UTOF. This UTOF value is the relative value and should be changed into the absolute values by Eq.(24).

$$\text{UTOF}_a = \text{UTOF} - 8\Delta t \tag{24}$$

where Δt is the cycle of sine pulse.

Finally, using the principle of ultrasonic thermometry, the average temperature T in the single path is determined.

The practical temperature is measured by thermocouple 1 and thermocouple 2 which are connected to digital temperature indicator MIK100 and digital temperature indicator XMT618, respectively.

Without and with heater source, in different distances from 5 cm to 40 cm (the environmental chamber is 55 cm wide), Fig. 13 shows the calculated temperature value and tested ones from digital

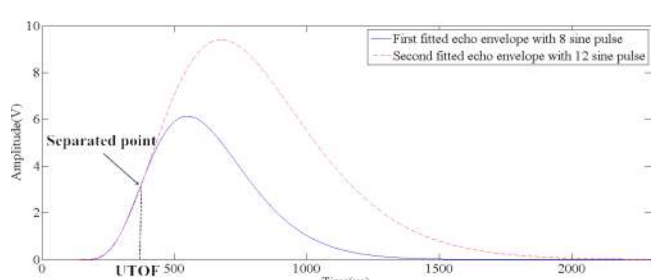

FIG. 12. The fitted echo envelopes with 8 and 12 sine wave pulses.

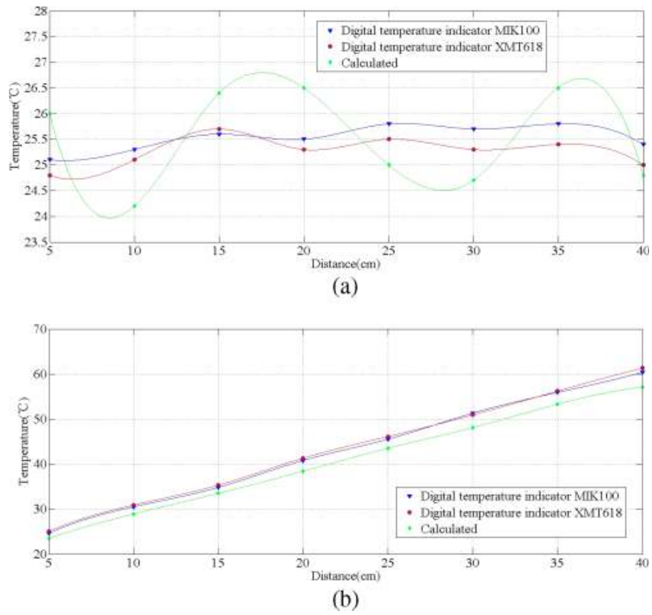

FIG. 13. Temperature values calculated and tested from indicators (a) Without heater source; (b) With heater source.

temperature indicator MIK100 and digital temperature indicator XMT618. Without heater source, the temperature measurement experiments are performed repeatedly for 50 times in every measure distance. Then, using the 50 calculated temperature values, the average value is gained. So, the calculated temperature in Fig. 13 is a mean value. But, with heater source, considering the speed of temperature rise, the temperature measurement experiments are performed repeatedly for 5 times in every measure distance.

The absolute error is defined as

$$E = \left| \frac{T - T_{mean}}{T_{mean}} \right| \times 100\% \tag{25}$$

$$T_{mean} = \frac{T_M + T_X}{2} \tag{26}$$

where T_M and T_X are the practical temperature values from digital temperature indicator MIK100 and digital temperature indicator XMT618. T is the calculated one.

Based on the data from Fig. 13, without heater source, the absolute error is between 1.59% and 4.33%. With heater source, the absolute error is between 4.42% and 6.46%. The absolute error with heater source is relatively higher than without heater source, since under the condition of heater source, transducers' properties are effected by heating environment. But, all errors are within the accepted range. The experimental results indicate ultrasonic thermometry has high precision.

V. CONCLUSION AND FUTURE WORK

Ultrasonic thermometry is an emerging area in thermometry and the accurate measurement of the UTOF is the key for ultrasonic temperature measurement. In this paper, we study the ultrasonic thermometry technique based on ultrasonic time-of-flight measurement by fitting the rising edges of double echo envelopes using double excitations with a pair of ultrasonic transducers for transmitting and receiving signal. Firstly, detailed description of principle of ultrasonic thermometry is given. And then, the algorithm of ultrasonic thermometry is shown. After that, experiments are carried out to study the algorithm performance. The experiment results show the errors between calculated temperature and tested ones from temperature indicators are within the accepted range, which means the ultrasonic thermometry has high precision.

The future work should be focused on multipath temperature measurement based on the single path temperature measurement. Then, for the special environment, like microwave heating, in order to know the information of temperature distribution, a two-dimension or three-dimension temperature field distribution may be obtained if multipath temperature measurement is completed.

ACKNOWLEDGMENT

This work is supported by Major State Basic Research Development Program (973 Program Grant no. 2013CB328903).

[1] G. Kychakoff, A. F. Hollingshead, and S. P. Boyd, "Use of acoustic temperature measurements in the cement manufacturing pyroprocess," in *Proceedings of the IEEE Cement Industry Technical Conference Record*, *May 2005*, pp. 23-33.
[2] K. Srinivasan, T. Sundararajan, and S. Narayanan, "Acoustic pyrometry in flames," Measurement **46**(1), 315-323 (2013).
[3] T. A. Hanson, N. Yilmaz, P. Drozda, W. Gill, T. J. Miller, and A. B. Donalson, "Acoustic pyrometry using an off-the-shelf range finding system," Journal of Fire Sciences **26**(4), 287-308 (2008).
[4] M. Bramanti, E. A. Salerno, A. Tonazzini, S. Pasini, and A. Gray, "An acoustic pyrometer system for tomographic thermal imaging in power plant boilers," IEEE Transactions on Instrumentation and Measurement **45**(1), 159-167 (1996).
[5] A. Kosugi, I. Ihara, and I. Matsuya, "Accuracy evaluation of surface temperature profiling by a laser ultrasonic method," Japanese Journal of Applied Physics **51**, 7 (2012).
[6] W.-Y. Tsai, H.-C. Chen, and T.-L. Liao, "High accuracy ultrasonic air temperature measurement using multi-frequency continuous wave," Sensors and Actuators A: Physical **132**(2), 526-532 (2006).
[7] A. Rathod, S. Mishra, S. Ghildiyal, and S. Mukhopadhyay, "Transform domain methods for performance enhancement of EFPI sensor," Sensors and Actuators, A: Physical **189**(99), 1-7 (2013).
[8] E. G. Sarabia, J. R. Llata, S. Robla, C. Torre-Ferrero, and J. P. Oria, "Accurate estimation of Airborne ultrasonic time-of-flight for overlapping echoes," Sensors **13**(11), 15465-15488 (2013).
[9] L. Angrisani, A. Baccigalupi, and R.S.L. Moriello, "A measurement method based on Kalman filtering for ultrasonic time-of-flight estimation," IEEE Transactions on Instrumentation and Measurement **55**(2), 442-448 (2006).
[10] R. Eberhart and J. Kennedy, "New optimizer using particle swarm theory," in *Proceedings of the International Symposium on Micromechatronics and Human Science*, *1995*. pp. 39-43.